Nonlinear wave propagation in a rapidly-spun fiber

C. J. McKinstrie and H. Kogelnik

Bell Laboratories, Lucent Technologies, Holmdel, New Jersey 07733, USA

mckinstrie@lucent.com

Abstract: Multiple-scale analysis is used to study linear wave propagation in a rapidly-spun fiber and its predictions are shown to be consistent with results obtained by other methods. Subsequently, multiple-scale analysis is used to derive a generalized Schroedinger equation for nonlinear wave propagation in a rapidly-spun fiber. The consequences of this equation for pulse propagation and four-wave mixing are discussed briefly.

OCIS codes: 060.4370 nonlinear optics, fibers; 190.4380, nonlinear optics, four-wave mixing; 190.5530 pulse propagation and solitons.

References and links

1. A. J. Barlow, J. J. Ramskov-Hansen and D. N. Payne, "Birefringence and polarization-mode dispersion in spun single-mode fibers," Appl. Opt. **20**, 2962–2968 (1981).
2. C. J. McKinstrie, S. Radic and A. R. Chraplyvy, "Parametric amplifiers driven by two pump waves," IEEE J. Sel. Top. Quantum Electron. **8**, 538–547 and 956 (2002).
3. J. Hansryd, P. A. Andrekson, M. Westlund, J. Li and P. O. Hedekvist, "Fiber-based optical parametric amplifiers and their applications," IEEE J. Sel. Top. Quantum Electron. **8**, 506–520 (2002).
4. S. Radic and C. J. McKinstrie, "Optical amplification and signal processing in highly-nonlinear optical fiber," IEICE Trans. Electron. **E88C**, 859–869 (2005).
5. R. M. Jopson and R. E. Tench, "Polarisation-independent phase conjugation of lightwave signals," Electron. Lett. **29**, 2216–2217 (1993).
6. K. Inoue, "Polarization independent wavelength conversion using fiber four-wave mixing with two orthogonal pump lights of different frequencies," J. Lightwave Technol. **12**, 1916–1920 (1994).
7. C. J. McKinstrie, H. Kogelnik, R. M. Jopson, S. Radic and A. V. Kanaev, "Four-wave mixing in fibers with random birefringence," Opt. Express **12**, 2033–2055 (2004).
8. T. Tanemura, K. Katoh and K. Kikuchi, "Polarization-insensitive asymmetric four-wave mixing using circularly polarized pumps in a twisted fiber," Opt. Express **13**, 7497–7505 (2005).
9. C. J. McKinstrie, J. D. Harvey, S. Radic and M. G. Raymer, "Translation of quantum states by four-wave mixing in fibers," Opt. Express **13**, 9131–9142 (2005).
10. J. P. Gordon and H. Kogelnik, "PMD fundamentals: Polarization mode dispersion in optical fibers," Proc. Nat. Acad. Sci. **97**, 4541–4550 (2000).
11. W. A. Shurcliff, *Polarized Light* (Harvard University Press, 1962).
12. P. McIntyre and A. W. Snyder, "Light propagation in twisted anisotropic media: Application to photoreceptors," J. Opt. Soc. Am. **68**, 149–157 (1978).
13. A. Galtarossa, P. Griggio, L. Palmieri and A. Pizzinat, "First- and second-order PMD statistical properties of constantly spun randomly birefringent fibers," J. Lightwave Technol. **22**, 1127–1136 (2004).
14. A. H. Nayfeh, *Introduction to Perturbation Techniques* (Wiley, 1981).
15. P. D. Maker and R. W. Terhune, "Study of optical effects due to an induced polarization third order in the electric field strength," Phys. Rev. **137**, A801–A818 (1965).
16. C. R. Menyuk, "Nonlinear pulse propagation in birefringent optical fibers," IEEE J. Quantum Electron. **23**, 174–176 (1987).
17. P. K. A. Wai, C. R. Menyuk and H. H. Chen, "Stability of solitons in randomly varying birefringent fibers," Opt. Lett. **16**, 1231–1233 (1991).
18. S. G. Evangelides, L. F. Mollenauer, J. P. Gordon and N. S. Bergano, "Polarization muliplexing with solitons," J. Lightwave Technol. **10**, 28–35 (1992).
19. U. Leonhardt, *Measuring the Quantum State of Light* (Cambridge University Press, 1997).

#72002 - $15.00 USD Received 15 June 2006; accepted 14 August 2006

1. Introduction

It has been known for many years that one can reduce the birefringence of an optical fiber by spinning it during the drawing process [1]. Spun fibers are used in interferometers and current (magnetic-field) sensors based on Faraday rotation, and as links in optical communication systems. One can also use spun fibers in parametric devices based on four-wave mixing (FWM).

There are three-types of FWM [2]: In the modulation instability (MI), which is driven by one pump wave, the signal wave is amplified and an idler wave is generated, which is a frequency-shifted and conjugated copy of the signal. In the phase-conjugation (PC) process, which is driven by two pumps, the signal is amplified and a frequency-shifted and conjugated idler is generated. In the frequency-conversion (FC) process, which is also driven by two pumps, the signal is not amplified. Instead, its power is transferred to an idler, which is a frequency-shifted, but non-conjugated copy of the signal. These processes have many uses in optical communication systems [3, 4].

Because transmission fibers (links) are not polarization-maintaining, parametric devices in communication systems must operate in the same way for all input-signal polarizations. PC driven by orthogonal (perpendicular) pumps in a highly-nonlinear fiber (HNF) provides amplification and conjugation that does not depend on the signal polarization [5, 6, 7]. In contrast, FC in a HNF depends sensitively on the signal polarization [7]. It was predicted recently that FC driven by co-rotating, circularly-polarized pumps in a rapidly-spun fiber (RSF) does not depend on the signal polarization [8, 9]. Although this prediction was validated approximately by an experiment [8], it was based on the idealization that a RSF behaves like a perfectly-isotropic fiber. The goal of this paper is to determine the conditions under which the theoretical predictions are accurate (and are likely to agree with other experimental results).

This paper is organized as follows: In Section 2 the transfer matrix associated with the propagation of a monochromatic wave through a uniformly-spun birefringent fiber is derived by solving the linear wave equation exactly. This transfer matrix is shown to be equivalent to the transfer matrix associated with a retarder followed by a rotator. The spatial evolution of the wave polarization is also determined. In Section 3 multiple-scale analysis (MSA) is used to reproduce the results of Section 2 approximately, for a RSF. This reproduction validates the perturbation method. Subsequently, in Section 4 MSA is used to derive a generalized Schroedinger equation (GSE) for nonlinear pulse propagation in a RSF. The implications of this equation for pulse propagation and FC are discussed briefly in Section 5. Finally, in Section 6 the main results of this paper are summarized.

2. Linear wave propagation

Let $A = [A_x, A_y]^t$ be the amplitude vector of a light wave. Then, in the absence of nonlinearity, the effects of propagation through a fiber are described by the input-output relation

$$A(z) = T(z)A(0). \tag{1}$$

At any distance z, the wave power $P = A^\dagger A$, where $\dagger$ denotes a hermitian conjugate. If the fiber is lossless, power is conserved. This condition requires that $T^\dagger T = I$: The transformation matrix T is unitary. The associated condition $|\det(T)| = 1$ implies that $\det(T) = e^{i\psi}$. If one defines $U = Te^{-i\psi/2}$, then $U^\dagger U = 1$ and $\det(U) = 1$: The modified transformation matrix U is unimodular. Physically, $\psi/2$ is the average phase shift of the polarization components, which we neglect, and U characterizes the changes in polarization, on which we focus. Unimodular transformations in Jones space, and the associated rotations in Stokes space, are reviewed in [10].

#72002 - $15.00 USD Received 15 June 2006; accepted 14 August 2006

The following discussion pertains to the reduced transformation

$$A(z) = U(z)A(0). \tag{2}$$

A unimodular matrix has 4 complex (8 real) coefficients. However, the conditions $U^\dagger U = I$ and $\det(U) = 1$ impose 5 real conditions on these coefficients, so only 3 real coefficients are independent. Hence, a unimodular matrix can be written in the (Cayley–Klein) form

$$U = \begin{bmatrix} \mu & \nu \\ -\nu^* & \mu^* \end{bmatrix}, \tag{3}$$

where the elements (transfer functions) μ and ν satisfy the auxiliary condition $|\mu|^2 + |\nu|^2 = 1$.

It is useful to review the transfer functions associated with some common optical devices. For a linear phase-shifter (retarder)

$$\mu = \cos(\phi_2) + i\sin(\phi_2)\cos(2\phi_1), \tag{4}$$
$$\nu = i\sin(\phi_2)\sin(2\phi_1), \tag{5}$$

where ϕ_1 is the angle between the ξ (slow) axis of the retarder and the x-axis (in the laboratory frame), and $\phi_2 = (\phi_\xi - \phi_\eta)/2$ is half the phase difference between amplitude components that are defined relative to the linearly-polarized eigenvectors $E_\xi = [1,0]^t$ and $E_\eta = [0,1]^t$ (in the retarder frame). For the special case in which $\phi_1 = 0$ (aligned retarder), Eqs. (4) and (5) reduce to $\mu = \exp(i\phi_2)$ and $\nu = 0$, respectively.

For a circular phase-shifter (rotator)

$$\mu = \cos(\phi_3), \tag{6}$$
$$\nu = \sin(\phi_3), \tag{7}$$

where $\phi_3 = (\phi_+ - \phi_-)/2$ is half the phase difference between amplitude components that are defined relative to the circularly-polarized eigenvectors $E_+ = [1,i]^t/2^{1/2}$ and $E_- = [1,-i]^t/2^{1/2}$. Equations (6) and (7) describe the (active) rotation of a linearly-polarized input vector through the angle $-\phi_3$.

For a retarder followed by a rotator, the composite transfer functions

$$\mu = \cos(\phi_2)\cos(\phi_3) + i\sin(\phi_2)\cos(2\phi_1 - \phi_3), \tag{8}$$
$$\nu = \cos(\phi_2)\sin(\phi_3) + i\sin(\phi_2)\sin(2\phi_1 - \phi_3). \tag{9}$$

This composite transformation is characterized by 3 real parameters (ϕ_1, ϕ_2 and ϕ_3). Hence, a unimodular transformation (transmission through a lossless fiber) is mathematically equivalent to transmission through a retarder followed by a rotator. This representation of fiber transmission is common in classical optics [11]. The composite transfer functions associated with a rotator followed by a retarder are also defined by Eqs. (8) and (9), with $2\phi_1 - \phi_3$ replaced by $2\phi_1 + \phi_3$. This alternative representation is also common in classical optics. Other concatenated transformations are described briefly in Appendix A.

For every unimodular transformation in Jones space there is an associated rotation in Stokes space. Despite their physical merits, Eqs. (8) and (9) do not provide a convenient mathematical link between Jones transformations and Stokes rotations. Fortunately, there is another approach. Let $\lambda_\pm$ be the eigenvalues of the Jones matrix U and let $E_\pm$ be the associated eigenvectors. Then the Jones matrix can be written in the canonical form

$$U = \lambda_+ E_+ E_+^\dagger + \lambda_- E_- E_-^\dagger. \tag{10}$$

#72002 - $15.00 USD Received 15 June 2006; accepted 14 August 2006

Two complex eigenvectors have 4 complex (8 real) components. However, the orthonormality relations $E_{\pm}^{\dagger}E_{\pm} = 1$ and $E_{\pm}^{\dagger}E_{\mp} = 0$ impose 4 real conditions on these components, and the phases of the eigenvectors are arbitrary, so only two of these components are independent: The eigenvectors can be written in the form

$$E_+ = [\cos(\theta_1/2)\exp(-i\theta_2/2), \sin(\theta_1/2)\exp(i\theta_2/2)]^t, \quad (11)$$

$$E_- = [-\sin(\theta_1/2)\exp(-i\theta_2/2), \cos(\theta_1/2)\exp(i\theta_2/2)]^t, \quad (12)$$

where θ_1 and θ_2 are real parameters. Because the eigenvalues have unit modulus, they can be written in the form $\lambda_{\pm} = \exp(\mp i\theta_3/2)$, where θ_3 is another real parameter. By using these definitions, one can write the canonical transfer matrix (10) in the form of Eq. (3), in which the transfer functions

$$\mu = \cos(\theta_3/2) - i\cos(\theta_1)\sin(\theta_3/2), \quad (13)$$

$$\nu = -i\sin(\theta_1)\sin(\theta_3/2)\exp(-i\theta_2). \quad (14)$$

Equations (13) and (14) are different from, but equivalent to, Eqs. (8) and (9).

For every Jones vector A there is an associated Stokes vector $\vec{A} = (A_1, A_2, A_3)$, where

$$A_1 = |A_x|^2 - |A_y|^2, \quad (15)$$

$$A_2 = A_x A_y^* + A_x^* A_y, \quad (16)$$

$$A_3 = i(A_x A_y^* - A_x^* A_y). \quad (17)$$

It follows from Eqs. (11) and (12), and Eqs. (15)–(17), that

$$\vec{E}_{\pm} = \pm(\cos\theta_1, \sin\theta_1\cos\theta_2, \sin\theta_1\sin\theta_2). \quad (18)$$

Equation (18) implies that θ_1 is the angle between $\vec{E}_+$ and 1-axis, and θ_2 is the angle between the projection of $\vec{E}_+$ on the 23-plane and the 2-axis: θ_1 and θ_2 are spherical polar coordinates in Stokes space. In [10] it is shown that the canonical transfer matrix (10) is associated with rotation about the axis $\vec{E}_+$ through the angle θ_3: Each parameter in representation (10) has a simple interpretation in Stokes space.

For example, by equating Eqs. (4) and (5) to Eqs. (13) and (14), one finds that $\theta_1 = 2\phi_1$, $\theta_2 = 0$ and $\theta_3 = -2\phi_2$: The retarder transformation corresponds to rotation about an axis, which lies in the 12-plane and is inclined at an angle $2\phi_1$ to the 1-axis, through the angle $-2\phi_2$ [rotation about the anti-parallel axis ($\theta_1 = \pi - 2\phi_1$ and $\theta_2 = \pi$) through the angle $2\phi_2$]. By equating Eqs. (6) and (7) to Eqs. (13) and (14), one finds that $\theta_1 = \pi/2$, $\theta_2 = \pi/2$ and $\theta_3 = -2\phi_3$: The rotator transformation corresponds to rotation about the positive 3-axis through the angle $-2\phi_3$ [rotation about the negative 3-axis ($\theta_1 = \pi/2$ and $\theta_2 = -\pi/2$) through the angle $2\phi_3$]. In general, the relations between the retarder-rotator parameters ϕ_1–ϕ_3 and the canonical parameters θ_1–θ_3 are complicated.

Now consider propagation through a spun birefringent fiber. If the fiber is spun during the drawing process, the finished fiber is stress free. It is customary to model such a fiber as a stack of infinitesimal birefringent plates, whose birefringence axes (ξ and η) are rotated by infinitesimal angles relative to those of the preceding plates [12]. In this model, the birefringence axes of the plate located at the distance z are rotated by the angle ρz relative to the coordinate axes of the laboratory (x and y). (As z increases, the tips of unit vectors parallel to the birefringence axes trace out right-handed screws.)

The rotating-frame amplitude vector is related to the laboratory-frame amplitude vector by the equation

$$A_r(z) = R(z)A_l(z), \quad (19)$$

#72002 - $15.00 USD Received 15 June 2006; accepted 14 August 2006

where the (passive) rotation matrix

$$R(z) = \begin{bmatrix} \cos(\rho z) & \sin(\rho z) \\ -\sin(\rho z) & \cos(\rho z) \end{bmatrix}. \tag{20}$$

In the rotating frame, the amplitude vector is governed by the equation

$$d_z A_r = L_r A_r, \tag{21}$$

where $d_z = d/dz$, the coefficient matrix

$$L_r = \begin{bmatrix} i\delta & \rho \\ -\rho & -i\delta \end{bmatrix}, \tag{22}$$

$\delta = (\beta_\xi - \beta_\eta)/2$ is the birefringence strength (half the wavenumber difference) and ρ is the rotation rate. (The birefringence beat-length is π/δ and the rotation length is $2\pi/\rho$.) The transfer matrix is the solution of the equation

$$d_z U_r = L_r U_r, \tag{23}$$

which is an extension of Eq. (21), subject to the boundary (initial) condition $U(0) = I$. By solving Eq. (23), one finds that the transfer functions

$$\mu_r(z) = \cos(kz) + i(\delta/k)\sin(kz), \tag{24}$$
$$\nu_r(z) = (\rho/k)\sin(kz), \tag{25}$$

where $k = (\delta^2 + \rho^2)^{1/2}$. If $\rho = 0$, $\mu_r(z) = \exp(i\delta z)$ and $\nu_r(z) = 0$, so the principal axes of the transformation are the birefringence axes of the fiber, and the phase difference between the principal amplitude components is $2\delta z$. Conversely, if $\delta = 0$, $\mu_r(z) = \cos(\rho z)$ and $\nu_r(z) = \sin(\rho z)$, so the Jones vector is rotated through an angle of $-\rho z$ relative to the birefringence axes of the fiber.

It follows from Eqs. (2) and (19) that the laboratory-frame transfer matrix is related to the rotating-frame transfer matrix by the equation

$$U_l(z) = R^\dagger(z) U_r(z). \tag{26}$$

By combining Eqs. (20) and (24)–(26), one finds that the transfer functions

$$\mu_l(z) = \cos(\rho z)\cos(kz) + (\rho/k)\sin(\rho z)\sin(kz) + i(\delta/k)\cos(\rho z)\sin(kz), \tag{27}$$
$$\nu_l(z) = (\rho/k)\cos(\rho z)\sin(kz) - \sin(\rho z)\cos(kz) + i(\delta/k)\sin(\rho z)\sin(kz). \tag{28}$$

If $\rho = 0$, $\mu_l(z) = \exp(i\delta z)$ and $\nu_l(z) = 0$: In the absence of spinning, the rotating frame coincides with the laboratory frame. Conversely, if $\delta = 0$, $\mu_l(z) = 1$ and $\nu_r(z) = 0$: In the absence of birefringence, the wave does not feel the effects of spinning, so the Jones vector is constant in the laboratory frame.

One can determine the parameters of the equivalent retarder-rotator by comparing Eqs. (24) and (25), or Eqs. (27) and (28), to Eqs. (8) and (9). In the rotating frame, one finds that

$$2\phi_1(z) = \tan^{-1}[\rho \tan(kz)/k] + n\pi, \tag{29}$$
$$\phi_2(z) = (-1)^n \sin^{-1}[\delta \sin(kz)/k], \tag{30}$$
$$\phi_3(z) = \tan^{-1}[\rho \tan(kz)/k]. \tag{31}$$

#72002 - $15.00 USD Received 15 June 2006; accepted 14 August 2006

Equations (29) and (31) reflect the fact that $2\phi_1 - \phi_3 = n\pi$. One can make ϕ_1 and ϕ_3 continuous by adding appropriate multiples of π at the appropriate distances.

The retarder parameters ϕ_1 and ϕ_2 have the same values in the laboratory frame as they do in the rotating frame. In contrast, the rotation parameter ϕ_3 is smaller by ρz, because two successive rotations through the angles $-\phi_3$ and ρz are equivalent to one rotation through the angle $-(\phi_3 - \rho z)$. It follows from Eq. (31) and the preceding statement that

$$\phi_3(z) = \tan^{-1}[\rho \tan(kz)/k] - \rho z. \tag{32}$$

Equations (29), (30) and (32) are equivalent to Eqs. (3), (1) and (2) of [1], respectively, which were based on the results of [12]. For a RSF ($|\rho| \gg |\delta|$), these equations imply that

$$2\phi_1(z) \approx \rho z, \tag{33}$$

$$\phi_2(z) \approx (\delta/k)\sin(kz), \tag{34}$$

$$\phi_3(z) \approx (\delta^2\rho/2k^3)[kz - \sin(2kz)/2], \tag{35}$$

where $k \approx \rho$ and $|\delta| \ll k$. Equations (33) and (34) are equivalent to Eqs. (11) and (9) of [1], respectively, and Eq. (35) is an improvement of Eq. (10) of [1]. Equation (33) implies that the slow axis of the equivalent retarder increases monotonically and rapidly with distance. However, Eq. (34) implies that $|\phi_2| \ll 1$, so the effects of the equivalent retarder are weak, and can be neglected. (Rapid spinning also reduces the polarization-mode dispersion of a randomly-birefringent fiber [13].) The rotation parameter of the equivalent rotator has a contribution that increases steadily and a contribution that oscillates. For long distances the latter contribution can be neglected: The effects of a RSF are equivalent to those of a rotator with $\phi_3(z) \approx \delta^2 z/2\rho$. One can obtain the same result from Eqs. (27) and (28). In the aforementioned limit, the transfer functions $\mu_l(z) \approx \cos[(k-\rho)z]$ and $\nu_l(z) \approx \sin[(k-\rho)z]$, which represent a rotation with the parameter $(k-\rho)z \approx \delta^2 z/2\rho$.

The laboratory-frame rotation angle $-\phi_3$ is plotted as a function of the distance parameter kz in Fig. 1, for the case in which the birefringence-to-spin ratio $\delta/\rho = 0.15$. The predictions of the approximate formula (35) are accurate.

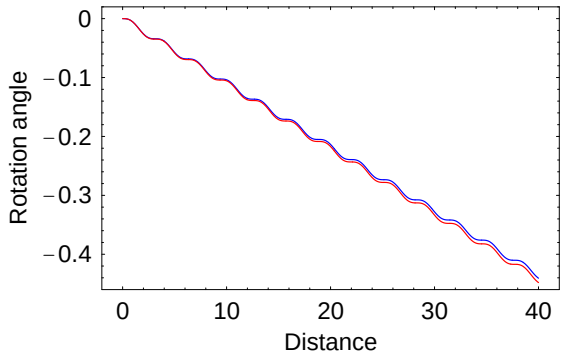

Fig. 1. Laboratory-frame rotation angle plotted as a function of distance for a birefringence-to-spin ratio of 0.15. The red curve represents the exact formula (32), whereas the blue curve represents the approximate formula (35).

One can visualize the wave evolution in Stokes space by combining Eqs. (24) and (25), or Eqs. (27) and (28), with definitions (15)–(17). The rotating-frame Stokes components are plotted as functions of the distance parameter kz in Fig. 2, for the case in which $\delta/\rho = 0.15$, and the trajectory of the rotating-frame Stokes vector is plotted in Fig. 3. By comparing Eqs.

#72002 - $15.00 USD Received 15 June 2006; accepted 14 August 2006

(24) and (25) to Eqs. (13) and (14), one finds that $\theta_1 = \tan^{-1}(-\rho/\delta)$, $\theta_2 = -\pi/2$ and $\theta_3 = 2kz$. The tip of the vector rotates about the axis $(-0.15, 0.00, -0.99)$, which is approximately equal to the negative 3-axis. In the rotating frame, the trajectory is simple.

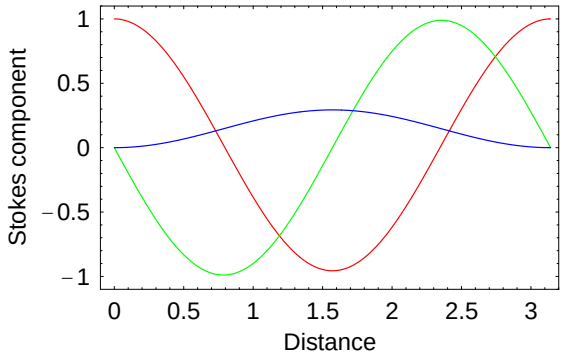

Fig. 2. Rotating-frame Stokes components plotted as functions of distance for a birefringence-to-spin ratio of 0.15. The red, green and blue curves represent the 1, 2 and 3 components, respectively.

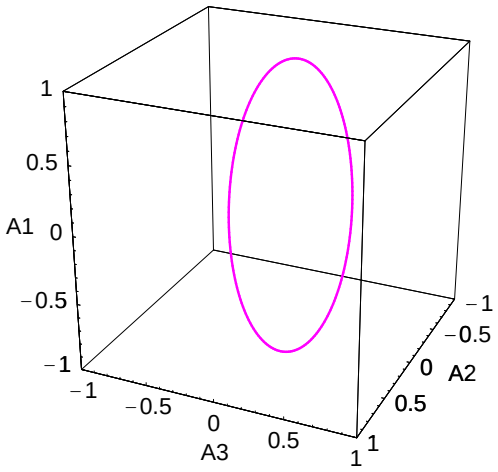

Fig. 3. Trajectory of the rotating-frame Stokes vector for a birefringence-to-spin ratio of 0.15.

The laboratory-frame Stokes components are plotted as functions of the distance parameter kz in Fig. 4, for the case in which $\delta/\rho = 0.15$, and the trajectory of the laboratory-frame Stokes vector is plotted in Fig. 5. The 3-component undergoes small, but fast, oscillations. In contrast, the 1- and 2-components undergo large, but slow, oscillations (on which are superposed the very small, but fast, oscillations that are required to conserve the length of the vector). Although the global transformation is complicated (as are the relations between the transfer functions and the canonical parameters), the associated local transformation (rate of change) is simple. Equations similar to (21) and (23) apply to the laboratory-frame amplitude vector A_l and transfer matrix U_l. It follows from (the laboratory-frame) Eq. (23) that

$$L_l(z) = d_z U_l(z) U_l^{\dagger}(z), \tag{36}$$

#72002 - $15.00 USD Received 15 June 2006; accepted 14 August 2006

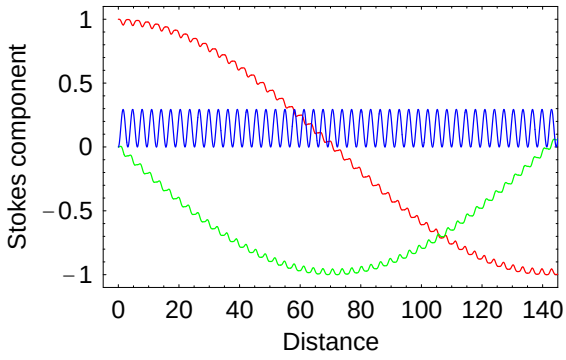

Fig. 4. Laboratory-frame Stokes components plotted as functions of distance for a birefringence-to-spin ratio of 0.15. The red, green and blue curves represent the 1, 2 and 3 components, respectively.

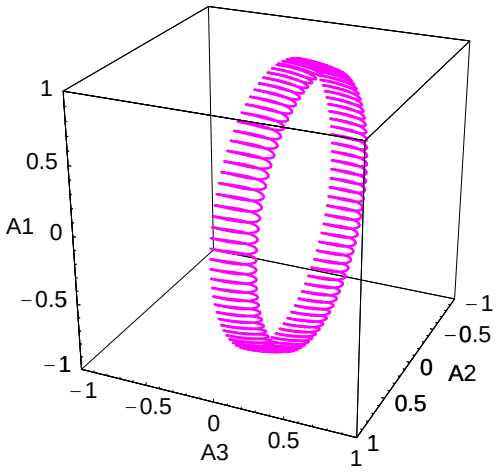

Fig. 5. Trajectory of the laboratory-frame Stokes vector for a birefringence-to-spin ratio of 0.15.

where U_l is known. By combining Eqs. (26) and (36) with the identity $R^\dagger R = I$, one obtains the alternative equation

$$L_l(z) = R^\dagger(z) L_r R(z) - R^\dagger(z) d_z R(z), \tag{37}$$

where R and L_r are known. It follows from either of the preceding equations that

$$L_l(z) = i\delta \begin{bmatrix} \cos(2\rho z) & \sin(2\rho z) \\ \sin(2\rho z) & -\cos(2\rho z) \end{bmatrix}. \tag{38}$$

In [10] it is shown that the coefficient matrix (38) is associated with rotation about the axis $-(\cos(2\rho z), \sin(2\rho z), 0)$ at the rate 2δ [rotation about the axis $(\cos(2\rho z), \sin(2\rho z), 0)$ at the rate -2δ]. In the laboratory frame, the trajectory is complicated because the rotation axis is not fixed: It rotates quickly about the 3-axis. The fast oscillations of the 3-component, which are evident in Figs. 4 and 5, are caused by the δ terms in Eqs. (27) and (28). If these contributions to the transfer functions are neglected, the tip of the vector rotates slowly about the negative 3-axis, as implied by the discussion that precedes Fig. 1.

#72002 - $15.00 USD Received 15 June 2006; accepted 14 August 2006

In summary, the effects of propagation through a RSF are described approximately by the laboratory-frame transfer matrix

$$U_l(z) = \begin{bmatrix} \cos(\delta^2 z/2\rho) & \sin(\delta^2 z/2\rho) \\ -\sin(\delta^2 z/2\rho) & \cos(\delta^2 z/2\rho) \end{bmatrix}. \tag{39}$$

This approximate transfer matrix is the solution of the equation

$$d_z U_l = L_l U_l, \tag{40}$$

where the approximate coefficient matrix

$$L_l = \begin{bmatrix} 0 & \delta^2/2\rho \\ -\delta^2/2\rho & 0 \end{bmatrix} \tag{41}$$

and the initial condition $U_l(0) = I$. Equations (39)–(41) describe the rotation of the Jones vector, with rate $-\delta^2/2\rho$. Their analogs in Stokes space describe rotation about the 3-axis, with rate $-\delta^2/\rho$.

3. Multiple-scale analysis of linear wave propagation

Typical single-mode fibers (SMFs) have beat lengths of order 10 m. In a recent FWM experiment with a twisted SMF [8], the twist length was of order 0.1 m. It is reasonable to consider spun fibers with comparable spin (rotation) lengths. Let ε denote the birefringence-to-spin ratio δ/ρ and ζ denote the distance variable ρz. Then, for the aforementioned RSFs, $\varepsilon \ll 1$ and one can rewrite the transfer functions (24) and (25) approximately as

$$\mu(\zeta) \approx \cos[(1+\varepsilon^2/2)\zeta] + i\varepsilon \sin[(1+\varepsilon^2/2)\zeta], \tag{42}$$

$$\nu(\zeta) \approx \sin[(1+\varepsilon^2/2)\zeta]. \tag{43}$$

It is convenient to work in the rotating frame, because the wave equation has constant coefficients in that frame. (The subscript r is omitted for simplicity of notation.) Formulas (42) and (43) are correct to order ε, and conserve power to order ε, for distances of order $1/\varepsilon$. One can also derive these formulas systematically, by using MSA [14].

Equations (21) and (22) imply that the propagation equation has the dimensionless form

$$DA = LA, \tag{44}$$

where the differential operator $D = d/d\zeta$, the amplitude vector $A = [A_\xi, A_\eta]^t$ and the matrix operator

$$L = \begin{bmatrix} i\varepsilon & 1 \\ -1 & -i\varepsilon \end{bmatrix}. \tag{45}$$

One can solve Eq. (44) perturbatively by writing $A = A_0 + \varepsilon A_1 + \varepsilon^2 A_2$ and $L = L_0 + \varepsilon L_1$, and introducing the independent distance scales ζ_0 and ζ_2, so that $D = D_0 + \varepsilon^2 D_2$, where $D_j = \partial/\partial\zeta_j$. By making these substitutions in Eq. (44), one finds that

$$(D_0 + \varepsilon^2 D_2)(A_0 + \varepsilon A_1 + \varepsilon^2 A_2) \approx (L_0 + \varepsilon L_1)(A_0 + \varepsilon A_1 + \varepsilon^2 A_2). \tag{46}$$

Equation (46) can be solved order-by-order in powers of ε, subject to the initial conditions $A_0(0) = A(0)$ and $A_n(0) = 0$ for $n \geq 1$.

The zeroth-order equation is

$$(D_0 - L_0)A_0 = 0, \tag{47}$$

#72002 - $15.00 USD Received 15 June 2006; accepted 14 August 2006

where

$$L_0 = \begin{bmatrix} 0 & 1 \\ -1 & 0 \end{bmatrix}. \tag{48}$$

The eigenvalues of L_0 are $\pm i$, and the associated eigenvectors $E_\pm$ are $[1,i]^t/2^{1/2}$ and $[1,-i]^t/2^{1/2}$, respectively, which correspond to (left and right) circularly-polarized eigenstates. Because the eigenvectors of L_0 are complete, one can write the zeroth-order amplitude in the form

$$A_0(\zeta_0,\zeta_2) = A_+(\zeta_0,\zeta_2)E_+ + A_-(\zeta_0,\zeta_2)E_-, \tag{49}$$

where the amplitude components

$$A_\pm(\zeta_0,\zeta_2) = \bar{A}_\pm(\zeta_2)\exp(\pm i\zeta_0). \tag{50}$$

At this stage, the dependences of $\bar{A}_\pm$ on ζ_2 are unknown.

The first-order equation is

$$(D_0 - L_0)A_1 = L_1 A_0, \tag{51}$$

where

$$L_1 = \begin{bmatrix} i & 0 \\ 0 & -i \end{bmatrix}. \tag{52}$$

By making the substitution

$$A_1(\zeta_0,\zeta_2) = B_+(\zeta_0,\zeta_2)E_+ + B_-(\zeta_0,\zeta_2)E_- \tag{53}$$

in Eq. (51), and using the facts that $L_1E_\pm = iE_\mp$, one finds that

$$(D_0 \mp i)B_\pm = i\bar{A}_\mp \exp(\mp i\zeta_0). \tag{54}$$

Equations (54) do not contain terms [proportional to $\exp(\pm i\zeta_0)$] that drive the first-order components $B_\pm$ resonantly, so their solutions

$$B_\pm(\zeta_0,\zeta_2) = i\bar{A}_\mp(\zeta_2)\sin(\zeta_0) \tag{55}$$

are bounded (and no ζ_1 is necessary).

The second-order equation is

$$(D_0 - L_0)A_2 = -D_2A_0 + L_1A_1. \tag{56}$$

By making the substitution

$$A_2(\zeta_0,\zeta_2) = C_+(\zeta_0,\zeta_2)E_+ + C_-(\zeta_0,\zeta_2)E_- \tag{57}$$

in Eq. (56), and using Eqs. (49), (50), (53) and (55), one finds that

$$(D_0 \mp i)C_\pm = -D_2\bar{A}_\pm \exp(\pm i\zeta_0) - \bar{A}_\pm \sin(\zeta_0). \tag{58}$$

The resonant contributions to the right sides of Eqs. (58) will be absent if

$$D_2\bar{A}_\pm = \pm i\bar{A}_\pm/2. \tag{59}$$

It follows from these conditions that

$$\bar{A}_\pm(\zeta_2) = \bar{A}_\pm(0)\exp(\pm i\zeta_2/2). \tag{60}$$

#72002 - $15.00 USD Received 15 June 2006; accepted 14 August 2006

To obtain a solution that is accurate to first order in ε, it is not necessary to calculate the bounded contribution to the second-order amplitude.

By combining the preceding formulas for A_0 and A_1, one finds that

$$\begin{aligned} A(z) \quad \approx \quad & \{\bar{A}_+(0)\exp[i(1+\varepsilon^2/2)z] + i\varepsilon\bar{A}_-(0)\sin(z)\}E_+ \\ & \{i\varepsilon\bar{A}_+(0)\sin(z) + \bar{A}_-(0)\exp[-i(1+\varepsilon^2/2)z]\}E_-. \end{aligned} \tag{61}$$

Equation (61) describes the approximate solution in terms of circularly-polarized basis vectors. By using the facts that $E_\pm = (E_\xi \pm iE_\eta)/2^{1/2}$, where $E_\xi = [1,0]^t$ and $E_\eta = [0,1]^t$, and the related facts that $\bar{A}_\pm(0) = [A_\xi(0) \mp iA_\eta(0)]/2^{1/2}$, one can rewrite Eq. (61) in the form

$$\begin{aligned} A(z) \quad \approx \quad & \{A_\xi(0)[\cos(kz) + i\varepsilon\sin(kz)] + A_\eta(0)\sin(kz)\}E_\xi \\ & \{-A_\xi(0)\sin(kz) + A_\eta(0)[\cos(kz) - i\varepsilon\sin(kz)]\}E_\eta, \end{aligned} \tag{62}$$

where $k \approx 1+\varepsilon^2/2$. Solution (62) is consistent with Eqs. (42) and (43). Hence, MSA reproduces the known results for linear wave propagation in a RSF. By continuing MSA to third order in ε, one can prove that the first-order amplitude has the same wavenumber correction as the zeroth-order amplitude. This extended analysis is described briefly in Appendix B.

4. Multiple-scale analysis of nonlinear pulse propagation

Now consider nonlinear pulse propagation in a RSF. In the rotating frame, the amplitude component A_ξ is governed by the generalized Schroedinger equation (GSE)

$$\partial_z A_\xi = i\delta A_\xi + \rho A_\eta - \beta_{1\xi}\partial_\tau A_\xi - i\beta_{2\xi}\partial^2_{\tau\tau}A_\xi/2 + N_\xi(A_\xi, A_\eta). \tag{63}$$

In Eq. (63) $\partial_z = \partial/\partial z$, $\partial_\tau = \partial/\partial\tau$, τ is the retarded time $t - sz$, where s is the polarization-averaged group slowness of the carrier wave, δ and ρ are the birefringence and spin coefficients, respectively, and β_1 and β_2 are the differential-convection and second-order dispersion coefficients $d\beta/d\omega - s$ and $d^2\beta/d\omega^2$, respectively, evaluated at the carrier frequency. The Kerr nonlinearity

$$N_\xi = i\gamma(|A_\xi|^2 A_\xi + 2|A_\eta|^2 A_\xi/3 + A^*_\xi A^2_\eta/3), \tag{64}$$

where γ is the Kerr coefficient, is based on the approximations that the nonlinear response is instantaneous and isotropic [15]. One obtains the equation for A_η from Eq. (63) by interchanging the subscripts ξ and η, and changing the signs of the birefringence, spin and convection terms ($\beta_{1\eta} = -\beta_{1\xi}$). To include the effects of higher-order dispersion, one replaces the second-order term $-\beta_2\partial_{\tau\tau}A/2$ by the Taylor expansion $\sum_{n\geq 2}\beta_n(i\partial_\tau)^n A/n!$.

In typical FWM experiments, the dephasing lengths (associated with dispersion) and mixing lengths (associated with nonlinearity) are of order 1 Km. To model FWM in RSFs, it is reasonable to assume that the spin, birefringence and mixing lengths have the ratios $1{:}10^2{:}10^4$. Similar ratios apply to the propagation of short intense pulses in RSFs. For such ratios, one can solve Eq. (63), and its analog for A_η, perturbatively. The spin terms in these GSEs are of order 1, the birefringence terms are of order ε, and the differential-convection, dispersion and nonlinearity terms are of order ε^2. (In this section the variables and parameters are dimensional, and ε is a book-keeping parameter.)

By proceeding as described in Section 3, one can write the GSEs in the matrix form

$$\begin{aligned} (D_0 + \varepsilon^2 D_2)(A_0 + \varepsilon A_1 + \varepsilon^2 A_2) \quad \approx \quad & (L_0 + \varepsilon L_1 + \varepsilon^2 L_2)(A_0 + \varepsilon A_1 \\ & + \varepsilon^2 A_2) + \varepsilon^2 N_2(A_0). \end{aligned} \tag{65}$$

#72002 - $15.00 USD Received 15 June 2006; accepted 14 August 2006

By defining the unitary matrices

$$I = \begin{bmatrix} 1 & 0 \\ 0 & 1 \end{bmatrix}, \; J = \begin{bmatrix} 1 & 0 \\ 0 & -1 \end{bmatrix}, \; K = \begin{bmatrix} 0 & 1 \\ -1 & 0 \end{bmatrix}, \tag{66}$$

one can write the zeroth- and first-order linear operators in the compact forms $L_0 = \rho K$ and $L_1 = i\delta J$, respectively. It is convenient to write the second-order linear operator in the form $L_2 = L_{2a} + L_{2d}$, where the average and half-difference operators

$$L_{2a} = -I(i\beta_{2a}\partial_{\tau\tau}^2/2), \tag{67}$$

$$L_{2d} = -J(\beta_{1d}\partial_\tau + i\beta_{2d}\partial_{\tau\tau}^2/2), \tag{68}$$

respectively, $\beta_a = (\beta_\xi + \beta_\eta)/2$ and $\beta_d = (\beta_\xi - \beta_\eta)/2$. The nonlinear vector

$$N_2 = i\gamma[2(A^\dagger A)A + (A^t A)A^*]/3. \tag{69}$$

Equation (65) can be solved order-by-order in powers of ε. Because the new (convection, dispersion and nonlinearity) terms are of second order, the zeroth- and first-order equations are equivalent to the corresponding equations in Section 3. The zeroth-order equations (and the analysis of Section 3) imply that

$$A_0(z_0, z_2) = A_+(z_0, z_2)E_+ + A_-(z_0, z_2)E_-, \tag{70}$$

$$A_\pm(z_0, z_2) = \bar{A}_\pm(z_2)\exp(\pm i\rho z_0), \tag{71}$$

and the first-order equations imply that

$$A_1(z_0, z_2) = B_+(z_0, z_2)E_+ + B_-(z_0, z_2)E_-, \tag{72}$$

$$B_\pm(z_0, z_2) = i\bar{A}_\mp(z_2)\delta\sin(\rho z_0)/\rho. \tag{73}$$

The second-order equation

$$(D_0 - L_0)A_2 = -D_2A_0 + L_1A_1 + L_2A_0 + N_2(A_0) \tag{74}$$

contains the basic terms $-D_2A_0$ and L_1A_1, like Eq. (56), and the extra terms L_2A_0 and $N_2(A_0)$, which were defined in Eqs. (67)–(69). It follows from Eqs. (72) and (73) that the second term

$$L_1A_1 = -[\delta^2\sin(\rho z_0)/\rho](\bar{A}_+E_+ + \bar{A}_-E_-). \tag{75}$$

Hence, the $+$ component has the resonant part $i(\delta^2/2\rho)\bar{A}_+\exp(i\rho z_0)$ and the nonresonant part $-i(\delta^2/2\rho)\bar{A}_+\exp(-i\rho z_0)$, which can be neglected. It follows from Eq. (67) that

$$L_{2a}A_0 = -(i\beta_{2a}\partial_{\tau\tau}^2A_+/2)E_+ - (i\beta_{2a}\partial_{\tau\tau}^2A_-/2)E_-. \tag{76}$$

Because A_+ is proportional to $\exp(i\rho z_0)$ [Eq. (71)], the whole $+$ component is resonant. It follows from Eq. (68) that

$$L_{2d}A_0 = -(\beta_{1d}\partial_\tau A_- + i\beta_{2d}\partial_{\tau\tau}^2A_-/2)E_+ - (\beta_{1d}\partial_\tau A_+ + i\beta_{2d}\partial_{\tau\tau}^2A_+/2)E_-. \tag{77}$$

Because A_- is proportional to $\exp(-i\rho z_0)$ [Eq. (71)], no part of the $+$ component is resonant, so the whole component can be neglected. It follows from Eq. (69) that

$$N_2 = i(2\gamma/3)(|A_+|^2 + 2|A_-|^2)A_+E_+ + i(2\gamma/3)(2|A_+|^2 + |A_-|^2)A_-E_-. \tag{78}$$

#72002 - $15.00 USD Received 15 June 2006; accepted 14 August 2006

Because $A_\pm$ is proportional to $\exp(\pm i\rho z_0)$, $|A_+|^2+2|A_-|^2$ is constant on the z_0-scale and the whole $+$ component is resonant. Similar statements can be made about the $-$ components in Eqs. (75)–(78). It follows from these observations that the resonant contributions to the right side of Eq. (74) will be absent if

$$\begin{aligned}\partial_{z_2}\bar{A}_\pm &= \pm i(\delta^2/2\rho)\bar{A}_\pm - i\beta_{2a}\partial_{\tau\tau}^2\bar{A}_\pm/2 \\ &\quad + i(2\gamma/3)(|\bar{A}_\pm|^2+2|\bar{A}_\mp|^2)\bar{A}_\pm. \end{aligned} \tag{79}$$

In the absence of dispersion and nonlinearity, Eqs. (79) reduce to Eqs. (59). It follows from Eqs. (71) and (79) that

$$\begin{aligned}\partial_z A_\pm &= \pm i(\rho+\delta^2/2\rho)A_\pm - i\beta_{2a}\partial_{\tau\tau}^2 A_\pm/2 \\ &\quad + i(2\gamma/3)(|A_\pm|^2+2|A_\mp|^2)A_\pm. \end{aligned} \tag{80}$$

Equations (80) apply to components that are defined relative to circularly-polarized basis vectors. By using the relations stated after Eq. (61), one finds that

$$\begin{aligned}\partial_z A_\xi &= (\rho+\delta^2/2\rho)A_\eta - i\beta_{2a}\partial_{\tau\tau}^2 A_\xi/2 \\ &\quad + i\gamma(|A_\xi|^2A_\xi+2|A_\eta|^2A_\xi/3+A_\xi^*A_\eta^2/3), \end{aligned} \tag{81}$$

where the components are defined relative to linearly-polarized basis vectors. By comparing Eq. (81) to Eqs. (63) and (64), one finds that rapid spinning eliminates differential convection and dispersion, for distances of order $1/\varepsilon^2$, but has no effect on the Kerr nonlinearity, which is intrinsically isotropic. One obtains the equation for A_η from Eq. (81) by interchanging the subscripts ξ and η, and changing the sign of the (rotation) coefficient $\rho+\delta^2/2\rho$.

Equations (80) and (81) are valid in the rotating frame. One obtains the laboratory-frame equations by removing the terms proportional to ρ, as explained in Section 2. By doing so, one obtains the vector GSE

$$\partial_z A = LA + i\beta_a(i\partial_\tau)A + i\gamma[2(A^\dagger A)A+(A^tA)A^*]/3, \tag{82}$$

where L is the rotation matrix defined by Eq. (41) and $\beta_a(i\partial_\tau)=\sum_{n\geq 2}\beta_{na}(i\partial_\tau)^n/n!$. The dispersion and nonlinearity terms have the same forms in the rotating and laboratory frames.

5. Discussion

By comparing Eq. (81) to Eq. (63), one finds that spinning a fiber rapidly suppresses the beating of the polarization components of the pulse, and their differential convection and dispersion, without affecting their nonlinear interaction. The only trace of birefringence and spinning that remains is polarization rotation at the (laboratory-frame) rate $-\delta^2/2\rho$. Because this rotation rate is the same for every frequency component of the pulse, the residual rotation has no significant effect on pulse propagation or FWM.

It is instructive to consider this result in detail. In a linearly-polarized basis, the residual effects of birefringence and spinning manifest themselves as slow rotation. Let L be the rotation matrix in Eq. (82) and let U be the solution of the equation $d_zU=LU$, subject to the boundary condition $U(0)=I$. Then, by making the substitution $A=UB$ in Eq. (82), and using the fact that $U^*=U$, one obtains the transformed vector GSE

$$\partial_z B = i\beta_a(i\partial_\tau)B + i\gamma[2(B^\dagger B)B+(B^tB)B^*]/3, \tag{83}$$

in which the effects of rotation are absent. Alternatively, in a circularly-polarized basis, the residual effects of birefringence and spinning manifest themselves as weak circular birefringence (wavenumber shifts $\pm\delta^2/2\rho$). By making the substitutions $A_\pm=B_\pm\exp(\pm i\delta^2 z/2\rho)$ in

#72002 - $15.00 USD Received 15 June 2006; accepted 14 August 2006

(the laboratory-frame) Eqs. (80), and using the fact that these scalar GSEs are incoherently-coupled ($|A_\pm|^2 = |B_\pm|^2$), one obtains transformed GSEs for $B_\pm$, in which the birefringence terms are absent.

The predictions of [8, 9], that FC driven by co-rotating pumps in a RSF does not depend on the signal polarization, were based on the assumptions that the linear response of the fiber is perfectly isotropic, and the nonlinear response is the full Kerr response (not modified by constant [16] or random [17, 18] birefringence). These physical assumptions led to a vector GSE that is mathematically equivalent to Eq. (83): Although the *a priori* omission of polarization rotation was not justified physically, the predictions made by the aforementioned GSE are correct.

If a fiber is twisted after the drawing process, the residual stress produces linear optical activity. One can model the effects of optical activity on pulse propagation by replacing the rotating-frame spin parameter ρ with the twist parameter $\rho - \alpha$, where $\alpha \approx 0.1\rho$ [1]. In the laboratory frame, slow polarization rotation at the rate $-\delta^2/2\rho$ is replaced by moderately-fast rotation at the rate $\alpha - \delta^2/2(\rho - \alpha)$. However, the rotation rate is still the same for every frequency component of the pulse. If one were to assume that the residual stress does not change the Kerr nonlinearity significantly, one would conclude that nonlinear pulse propagation and FWM in a rapidly-twisted fiber are similar to propagation and FWM in a RSF. This conclusion is consistent with the results of a recent experiment [8].

6. Summary

In this paper, multiple-scale analysis was used to derive a generalized Schroedinger equation that models optical pulse propagation in a rapidly-spun fiber [Eq. (82)]. This analysis was based on the assumption that (apart from the carrier wavelength of the pulse) the shortest length scale is the spin length, the intermediate scale is the birefringence beat-length, and the longest scale is the (common) dispersion and nonlinearity length. Because spinning rotates the birefringence axes of the fiber rapidly, the effects of birefringence (beating, differential convection and differential dispersion of the polarization components) are reduced significantly. In contrast, spinning does not change the nonlinear (Kerr) response of the fiber. For distances of interest, the only trace of birefringence and spinning that remains is the slow rotation of the pulse polarization. Because the rotation rate is the same for every frequency component of the pulse, this residual rotation has no significant effect on pulse propagation or four-wave mixing: Previous predictions [8, 9], that frequency-conversion driven by co-rotating pumps in a rapidly-spun fiber does not depend on the signal polarization, are correct.

Acknowledgment

We thank L. Schenato for his constructive comments on the manuscript.

Appendix A: Other concatenated transformations

In Section 2, wave propagation through a lossless fiber was shown to be equivalent to wave propagation through a nonaligned retarder and a rotator. This equivalence exists because the transfer matrix of the fiber can be written as the product of the transfer matrices associated with the aforementioned devices. The transfer matrix of the fiber can be decomposed in other ways. For example, the composite transfer functions associated with a rotator, located between two aligned retarders, are

$$\mu = \cos(\phi_2)\exp[i(\phi_3 + \phi_1)], \tag{84}$$

$$\nu = \sin(\phi_2)\exp[i(\phi_3 - \phi_1)], \tag{85}$$

#72002 - $15.00 USD Received 15 June 2006; accepted 14 August 2006

where ϕ_2 is the rotation parameter (half phase-difference) associated with the rotator ($-\phi_2$ is the rotation angle), and ϕ_1 and ϕ_3 are the phase shifts (half phase-differences) associated with the initial and final retarders, respectively. Because the composite transformation is characterized by three real parameters, it is mathematically equivalent to transmission through a fiber. This representation of fiber transmission is common in quantal optics [19], because the rotator transfer functions (6) and (7) are the same as those for a beam-splitter, whose properties are well known.

By comparing Eqs. (84) and (85) with Eqs. (24) and (25), one finds that

$$\phi_1 = \tan^{-1}[\delta \tan(kz)/k]/2, \tag{86}$$

$$\phi_2 = \sin^{-1}[\rho \sin(kz)/k] \tag{87}$$

and $\phi_3 = \phi_1$. These results are valid in the rotating frame. One can convert them to laboratory-frame results by multiplying the transfer matrix associated with Eqs. (84) and (85) by the transfer matrix associated with a rotation through the angle ρz. However, because the last transformation associated with Eqs. (84) and (85) is a retardation, rather than a rotation, the laboratory-frame results are complicated. In the present context, the nonaligned retarder–rotator representation of fiber transmission is more convenient.

Appendix B: Third-order multiple-scale analysis

In Section 3 it was shown that the zeroth- and first-order amplitudes can be written in the forms of Eqs. (49) and (53), respectively, where the amplitude components $A_\pm$ and $B_\pm$ satisfy Eqs. (50) and (54). The first-order equations have the solutions

$$B_\pm(\zeta_0,\zeta_2) = \pm[\bar{B}_\pm(\zeta_2)\exp(\pm i\zeta_0) - \bar{A}_\mp(\zeta_2)\exp(\mp i\zeta_0)]/2, \tag{88}$$

where $\bar{B}_\pm(0) = \bar{A}_\mp(0)$. At this stage, the dependences of $\bar{B}_\pm$ on ζ_2 are unknown. If one makes the *a priori* assumptions that $\bar{B}_\pm(\zeta_2) = \bar{A}_\mp(\zeta_2)$, which are consistent with the initial conditions, then Eqs. (88) reduce to Eqs. (55). However, these assumptions are unnecessarily restrictive.

The second-order amplitude can be written in the form of Eq. (57), where the components $C_\pm$ satisfy the equations

$$(D_0 \mp i)C_\pm = -D_2\bar{A}_\pm \exp(\pm i\zeta_0) \mp i[\bar{B}_\mp \exp(\mp i\zeta_0) - \bar{A}_\pm \exp(\pm i\zeta_0)]/2. \tag{89}$$

The resonant contributions to the right sides of Eqs. (89) will be absent if

$$D_2\bar{A}_\pm = \pm i\bar{A}_\pm/2. \tag{90}$$

It follows from these conditions that

$$\bar{A}_\pm(\zeta_2) = \bar{A}_\pm(0)\exp(\pm i\zeta_2/2). \tag{91}$$

Equations (90) and (91) are identical to Eqs. (59) and (60), respectively. It follows from Eqs. (89) that the bounded contributions to the second-order components are

$$C_\pm(\zeta_0,\zeta_2) = -[\bar{C}_\pm(\zeta_2)\exp(\pm i\zeta_0) - \bar{B}_\mp(\zeta_2)\exp(\mp i\zeta_0)]/4, \tag{92}$$

where $\bar{C}_\pm(0) = \bar{B}_\mp(0)$.

The third-order equation is

$$(D_0 - L_0)A_3 = -D_2A_1 + L_1A_2. \tag{93}$$

#72002 - $15.00 USD Received 15 June 2006; accepted 14 August 2006

By making the substitution

$$A_3(\zeta_0,\zeta_2) = D_+(\zeta_0,\zeta_2)E_+ + D_-(\zeta_0,\zeta_2)E_- \tag{94}$$

in Eq. (93), one finds that

$$\begin{aligned}(D_0 \mp i)D_\pm &= \mp D_2[\bar{B}_\pm \exp(\pm i\zeta_0) - \bar{A}_\mp \exp(\mp i\zeta_0)]/2 \\ &\quad - i[\bar{C}_\mp \exp(\mp i\zeta_0) - \bar{B}_\pm \exp(\pm i\zeta_0)]/4.\end{aligned} \tag{95}$$

The resonant contributions to the right sides of Eqs. (95) will be absent if

$$D_2\bar{B}_\pm = \pm i\bar{B}_\pm/2. \tag{96}$$

It follows from these conditions, and the initial conditions stated after Eqs. (88), that

$$\bar{B}_\pm(\zeta_2) = \bar{A}_\mp(0)\exp(\pm i\zeta_2/2). \tag{97}$$

By combining Eqs. (88) and (97), one finds that

$$B_\pm(\zeta_0,\zeta_2) = iA_\mp(0)\sin(\zeta_0 + \zeta_2/2), \tag{98}$$

as stated in Section 3.

#72002 - $15.00 USD Received 15 June 2006; accepted 14 August 2006